

Effect of crystal size reduction on lattice symmetry and cooperative properties

Pushan Ayyub, V. R. Palkar, Soma Chattopadhyay, and Manu Multani

Materials Research Group, Tata Institute of Fundamental Research, Homi Bhabha Road, Bombay 400 005, India

(Received 21 October 1994)

Size-induced changes in the crystal symmetry have been observed in Al_2O_3 , Fe_2O_3 , PbTiO_3 , PbZrO_3 , $\text{La}_{1.85}\text{Sr}_{0.15}\text{CuO}_4$, $\text{YBa}_2\text{Cu}_3\text{O}_{7-\delta}$, and $\text{Bi}_2\text{CaSr}_2\text{Cu}_2\text{O}_8$. In these systems—and presumably in a large majority of partially covalent oxides—the crystal lattice tends to transform into a structure of *higher symmetry* with a decrease in the crystal size. We also find that the size dependence of many important physical properties can be ascribed directly to the lattice distortion. The physical mechanism responsible for these phenomena is intriguing and their complete understanding essential since they effectively define the practical lower limit to the miniaturization of devices based on these materials.

I. INTRODUCTION

Most physical and chemical properties of solid matter change when the particle size is decreased to the submicrometer regime. From the body of available data it appears that these changes can be attributed to one or more of the following sources. (a) *Quantum size effects*. The electronic energy spectrum in small particles is quantized into discrete levels with a level spacing (near the Fermi energy ϵ_F) $\Delta = \epsilon_F/N$, where N is the (now noninfinite) number of electrons. Quantum size effects¹ appear when the particles are small enough for Δ to be comparable to the characteristic energy parameters (kT , $\hbar\omega$, μH , etc.). (b) *Surface and interface effects*. The relative number of atoms at the surfaces and interfaces increases with decreasing size, making surface effects very important in small solids. The properties of intergranular matter are often vastly different from normal bulk matter.² (c) *Changes in the cell parameters and lattice symmetry*. With a decrease in the particle size, the lattice constants exhibit a regular change (an expansion for most nonmetallic solids). These changes are small but often lead to important modifications in many physical properties. While the first two aspects, (a) and (b), have been comparatively better studied, we report one of the few investigations of the third aspect. The stability of a crystal and the equilibrium lattice parameters are controlled by a local balance between short-range repulsive forces and long-range Coulomb forces. Since short-range forces are governed almost entirely by near-neighbor interactions, the influence of crystal size on them should be negligible. Long-range forces and cooperative phenomena, on the other hand, should be more affected by size effects.

That a reduction in the physical dimension of a crystal lattice leads to changes in the lattice constants was recognized as far back as 1930, when Lennard-Jones³ made the conjecture that the unit cell should contract with decreasing size in ionic systems and expand in covalent ones. This turned out to be an oversimplification, but in spite of some progress⁴ in recent years the problem has eluded complete understanding. Drawing a simple analogy with a liquid drop and invoking the Laplace pressure, $4\gamma/d$ (γ =surface tension, d =particle diameter) is improper because it is difficult to completely decouple surface and volume stresses in a

solid and make an unambiguous choice for the value of γ . Moreover, surface-tension-like forces would *always* lead to a lattice contraction in small particles which is contrary to many observations.

We show that the variation of the lattice constants with particle size follows certain well-defined trends in a large number of partially covalent oxides. In all such cases, we observe an expansion of the unit cell with reduction in particle size. The expansion is anisotropic and the lattice almost invariably becomes *more symmetric* as the size is decreased. The samples studied belong to the perovskite and corundum families and include technologically important systems such as ferroelectrics, ferromagnets, superconductors, and structural ceramics. Though the size-induced lattice distortions are relatively small in magnitude, they lead to profound changes in many physical properties and tend to destroy the cooperative long-range order in the systems mentioned above. Thus we observe large deviations in the T_c , the order parameter, and related properties with respect to the corresponding bulk solid when the size is decreased to 10–100 nm.

In a few cases, size effects may be large enough to cause a structural transition—to a phase with a more symmetric structure. This was first recognized⁵ in Fe_2O_3 where a decrease in size below 30 nm was found to alter the equilibrium crystal structure from the corundum to the inverse spinel type. It had been earlier observed⁶ that the normally unquenchable high-temperature tetragonal phase of ZrO_2 becomes stable at room temperature when the particle size is less than 10 nm. Since bulk ZrO_2 has monoclinic symmetry, this observation can be interpreted as a size-driven monoclinic→tetragonal structural transition. More recently, the tetragonal ferroelectric phase of BaTiO_3 was found to convert to the cubic paraelectric phase at room temperature below a critical particle size.⁷ Size-induced changes in the crystal symmetry have also been observed⁸ in $\text{YBa}_2\text{Cu}_3\text{O}_{7-\delta}$ and $\text{Bi}_2\text{CaSr}_2\text{Cu}_2\text{O}_8$. In both cases the orthorhombic structure changes continuously to a tetragonal one with a decrease in size. The decrease in the orthorhombic distortion is accompanied by a reduction in the superconducting T_c . To establish the generality of this phenomenon, we have studied it in different classes of oxides.

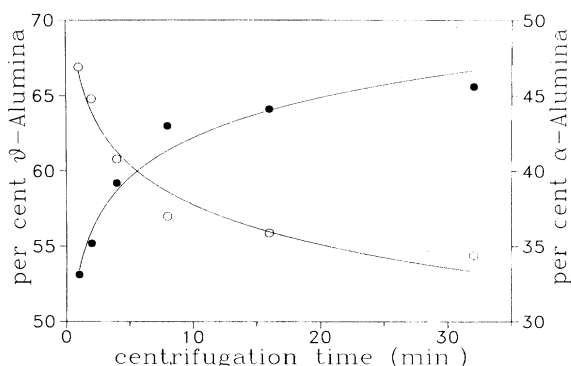


FIG. 1. Change in the phase fractions of α - Al_2O_3 (open circles) and θ - Al_2O_3 (closed circles) with centrifugation time.

II. RESULTS

A. Al_2O_3 and Fe_2O_3

Alumina (Al_2O_3) occurs in a number of different structural modifications, such as α (rhombohedral corundum structure), γ (cubic), δ (tetragonal), θ (monoclinic), etc. From a systematic study of the pyrolysis products of an oxy-alkoxy precursor, Morgan *et al.*⁹ determined the following stability ranges for the different phases: γ - Al_2O_3 ($<600^\circ\text{C}$), θ - Al_2O_3 (600 – 1000°C), and α - Al_2O_3 ($>1000^\circ\text{C}$). This study pertained to the mixed phase system: $\text{Al}_2\text{O}_3 + 10\% \text{ZrO}_2$. We have made a systematic study of the inter-relation of the phase stability and particle size in pure Al_2O_3 .

Nanocrystalline alumina with different average particle sizes was prepared by the sol-gel process. Ultrafine Böhmite, $\text{AlO}(\text{OH})$, was first synthesized by the action of deionized water on amalgamated aluminum. A stable aqueous suspension (sol) was formed by adding a few drops of acetic acid and peptizing at 80°C for 15 min. The sol was gelled with a dehydrating agent (2-ethyl hexanol) in the presence of a surfactant (Span 80). The gel was dried and calcined at different temperatures to obtain alumina. The inevitable particle size distribution in the product was narrowed down considerably by a size fractionation procedure using a pipette centrifuge (Ladal Analysette Model 21.002). This instrument—normally used for the measurement of particle size distribution—consists of a shallow stainless steel bowl which holds the sample in the form of a suspension. The bowl is rotated about its central axis at speeds up to 1500 rpm and size separation occurs during the centrifugal motion. Samples are sucked out at specified time intervals from points at a fixed distance from the axis. The samples collected at different times were dried and analyzed for particle size and chemical phase.

The as-prepared sample (calcined at 1100°C for 30 min) consists of a mixture of mainly α and θ phases with a small amount of δ phase. Note that during fractionation, samples extracted after longer times have smaller mean size. The changes in the fraction of α and θ phases with centrifugation time is shown in Fig. 1. Clearly, smaller particles (longer times) are more likely to be θ - Al_2O_3 , and larger particles, α - Al_2O_3 . Even smaller particles (samples calcined at or below 650°C) belong to the γ phase.

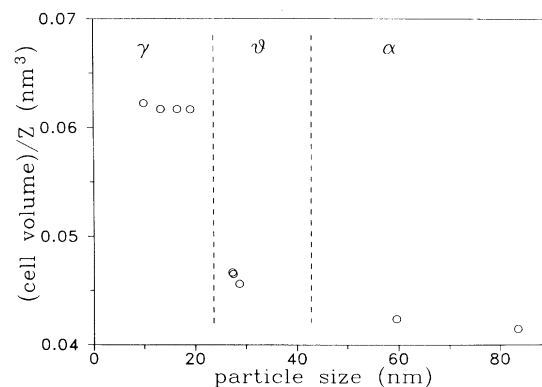


FIG. 2. Normalized unit cell volume as a function of the x-ray domain size for different phases (α , θ , and γ) of Al_2O_3 .

We now consider the changes in the unit cell volume (UCV) with decreasing size. A valid comparison of the UCV of different crystallographic phases can be made when the UCV is normalized with respect to the number of formula units per unit cell (Z) for each phase. The “particle size” is the volume averaged size of the coherently diffracting domains obtained from x-ray diffraction line broadening after making the usual correction for instrumental broadening. Figure 2 shows that the UCV increases with decreasing size for each phase. The crossover from one phase to another with decreasing size is accompanied by large, discontinuous increases in the UCV. A similar size-induced structural transition was earlier observed⁵ in the case of Fe_2O_3 . The normalized UCV vs particle size data for the α and γ phases of Fe_2O_3 (Fig. 3) resemble the results obtained for Al_2O_3 . In both Fe_2O_3 and Al_2O_3 , the same sequence of structural transitions is known to occur as a function of temperature. Our data therefore suggest that in certain physical situations, size can play the role of a thermodynamic parameter. Expressed graphically in an imaginary “phase diagram” (Fig. 4), this means that the same structural phase transitions ($A \rightarrow B \rightarrow C$) can be induced by changing either temperature or size ($\sim N^{1/3}$, where N is equal to the number of atoms per particle). In practice, the situation is often complicated by the fact that an increase in temperature may lead to an increase in size due to agglomeration and growth of compacted or loosely aggregated grains.

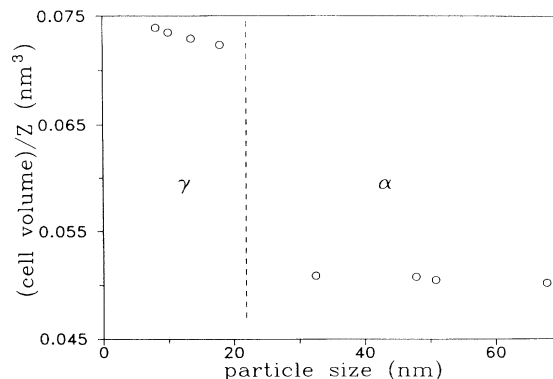


FIG. 3. Normalized unit cell volume as a function of the x-ray domain size for different phases (α and γ) of Fe_2O_3 .

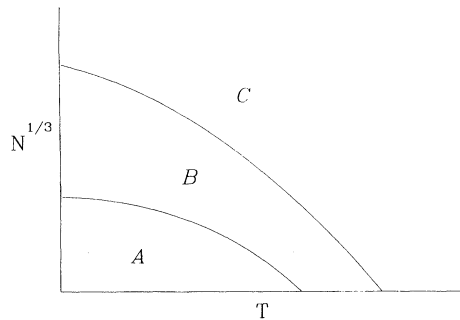


FIG. 4. Generalized phase diagram of a system with three crystallographic phases: A, B, and C. The coordinates are size ($\sim N^{1/3}$) and temperature T .

B. PbTiO_3 and PbZrO_3

PbTiO_3 is a model displacive ferroelectric with a tetragonal perovskite structure ($a=0.3899$ nm, $c=0.41532$ nm, $c/a=1.065$) at room temperature. Above $T_c=763$ K, it transforms to a cubic ($a=c=0.396$ nm) paraelectric structure with each Ti^{4+} ion at the center of an oxygen octahedron. Below T_c , the softening of a TO mode causes an off-center displacement of the Ti^{4+} ion by 17 pm along the polar axis (with the Pb^{2+} ion as origin) and, consequently, a spontaneous polarization, P_S . The tetragonal distortion (c/a), therefore, scales as the order parameter (P_S).

Ultrafine particles of PbTiO_3 were prepared by coprecipitation as hydroxides from a solution of $\text{Pb}(\text{NO}_3)_2$ and $\text{Ti}(\text{NO}_3)_4$. The dried precipitate was heated at various temperatures between 450 °C and 900 °C to obtain PbTiO_3 particles with average sizes in the range of 45–300 nm. The ferroelectric transition temperature was determined by measuring the temperature dependence of the static dielectric response function as well as by differential scanning calorimetry. Both techniques show a progressive reduction in the transition temperature and a broadening of the transition width with a reduction in size. Also, Fig. 5 shows that a reduction in size results in a decrease of the tetragonal distortion (c/a) which appears to be correlated to the reduction in T_c .

Size effects in ferroelectrics have recently been investigated from the point of view of the phenomenological

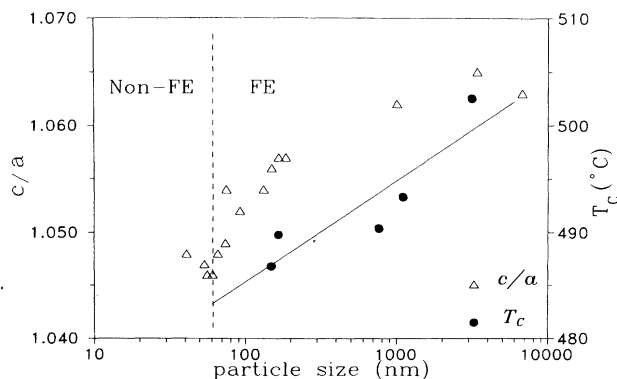


FIG. 5. Dependence of the tetragonal distortion, c/a (triangles) and ferroelectric T_c (circles) with particle size in PbTiO_3 . The T_c vs size variation has been fitted with a straight line. No ferroelectric (FE) transition is observed below ≈ 60 nm.

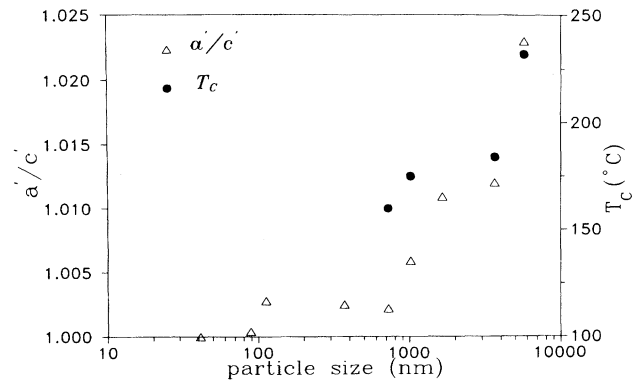


FIG. 6. Dependence of the pseudotetragonal distortion a'/c' (triangles) and antiferroelectric T_c (circles) with the particle size in PbZrO_3 . The pseudotetragonal cell constants (a', c') are related to the orthorhombic cell constants as $a' = a/\sqrt{2} = b/2\sqrt{2}$ and $c' = c/2$.

Landau-Devonshire theory¹⁰ as well as that of the soft-mode approach.¹¹ The spontaneous polarization is predicted to go smoothly to zero at some critical size. Our results, however, indicate that the initial reduction in T_c may be caused by the size-induced modification of the structure towards the cubic symmetry. Note that the ferroelectric transition is not observed below a size of ≈ 60 nm, in spite of a still nonzero tetragonal distortion. The balance between the short-range repulsive and the long-range attractive forces (necessary for the softening of a lattice mode) appears to be affected in the latter size regime, leading to an abrupt disappearance of ferroelectricity.

PbZrO_3 is antiferroelectric at room temperature and has an orthorhombic structure. Transition to a cubic, paraelectric phase occurs at 230 °C. Fine particles of PbZrO_3 were prepared by a modified sol-gel technique starting with an aqueous solution of $\text{ZrOCl}_2 \cdot 8\text{H}_2\text{O}$ and $\text{Pb}(\text{NO}_3)_2$. Figure 6 shows that the pseudotetragonal lattice distortion in the antiferroelectric phase decreases monotonically to 1 with decreasing size. As in the case of PbTiO_3 , the T_c appears to scale with the pseudotetragonal distortion.

C. $\text{La}_{1.85}\text{Sr}_{0.15}\text{CuO}_4$

Bulk $\text{La}_{1.85}\text{Sr}_{0.15}\text{CuO}_4$ (LSCO), which is tetragonal at room temperature, undergoes a superconducting transition below $T_c=36$ K. Submicrometer particles were synthesized by rapid liquid dehydration. The process involved a fast nucleation of fine particles from a mixture of the citrates of La, Sr, and Cu in aqueous solution. Dry acetone was used as dehydrating agent since it has a high solubility for water but not for the metal salts. The citrate precipitate was calcined at different temperatures to obtain samples with different average sizes. The superconducting transition was studied by a superconducting quantum interference device magnetometer (Quantum Design). Figure 7 shows that both the tetragonal distortion (c/a) and T_c fall monotonically with decreasing size below ≈ 0.6 μm .

The basic structural units of LSCO are the corner-sharing CuO_6 octahedra, which form a two-dimensional layered structure. A Jahn-Teller (JT) distortion of these octahedra splits the degenerate e_g levels of the $\text{Cu}(3d)$ states. A de-

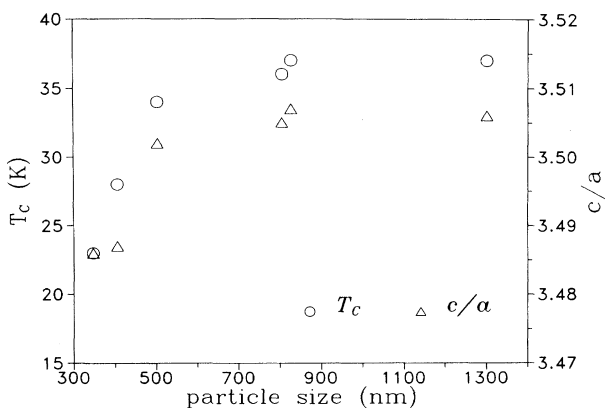


FIG. 7. Dependence of the superconducting T_c (circles) and the tetragonal (Jahn-Teller) distortion c/a (triangles) in $\text{La}_{1.85}\text{Sr}_{0.15}\text{CuO}_4$.

crease in size is seen to reduce the JT distortion. The strong correlation between the extent of the JT distortion and the T_c that we observe appears to underline the importance of the JT effect in the mechanism of superconductivity in this class of high- T_c superconductors. Such a connection was suggested by Bednorz and Müller in their landmark paper,¹² and in fact formed the basis for their search for superconductivity in cuprates and nickelates.

III. DISCUSSIONS

Even though a typical transition-metal oxide such as Fe_2O_3 is largely ionic, the interionic bonds are known to have a directional character. It follows that there would be unpaired electronic orbitals at the outer surface of each particle. This roughly parallel array of surface dipoles would repel each other and result in a larger value of the equilibrium lattice constant than in the bulk crystal.

Why is it that the lattice expansion is usually found to be anisotropic? In a typical transition-metal oxide, the magnitude of the interaction between the $3d$ electron of the metal and the oxygen nucleus is an approximate measure of the covalence.¹³ A measurement of the pressure dependence of

the Racah parameters (which are different combinations of the Condon-Shortley integrals in crystal field theory) confirms that the covalence (as defined above) increases with increasing pressure. We have shown that for a large class of partially covalent oxides, a decrease in the particle size has the same effect as the application of a *negative* pressure. We therefore expect these systems to become increasingly ionic with decreasing size. Consequently, the interionic bonds would lose their directional character and the crystal would tend to assume a structure with comparatively higher symmetry. It is interesting to note, in this context, that *strongly covalent* systems such as Si or Ge do not undergo any structural distortion even when the size is decreased to ≈ 10 nm.¹⁴ In such systems, size-induced equivalent pressures are probably not large enough to induce appreciably ionic character.

In a significant number of the oxides studied, there is a change in the oxygen stoichiometry in the nanocrystalline samples. In all the high- T_c oxides, the oxygen number decreases with decreasing size. In $\alpha\text{-Fe}_2\text{O}_3$ and $\alpha\text{-Al}_2\text{O}_3$, a reduction in size leads to a transition to an oxygen deficient crystal structure (the corresponding γ phases) without, however, any change in the cation:oxygen ratio.

Finally, on reviewing our data on size effects in oxides, we arrive at the somewhat unexpected conclusion that in many important cases, deviations from bulk properties are related primarily to the changes in the size and symmetry of the unit cell. The significance of this finding is that it provides an insight into the delicate interplay between the structure and properties of solid matter. The crucial role of interatomic distance in solid state physics has been established from high pressure research. This is reiterated by size effect studies since the lattice parameter is a function of particle size. Further, it may lead to methods for stabilizing normally unstable or metastable high-symmetry structures such as cubic ZnO.

ACKNOWLEDGMENTS

We thank Professor R. Vijayaraghavan for supporting and encouraging the small solids program and acknowledge the expert technical help provided by R. M. Wankar and A. V. Gurjar.

¹R. Kubo, J. Phys. Soc. Jpn. **17**, 975 (1962).

²H. Gleiter, Nanostructured Materials **1**, 1 (1992).

³J. E. Lennard-Jones, Z. Crystallogr. **75**, 215 (1930).

⁴M. Ya. Gamarnik, Phys. Status Solidi B **178**, 59 (1993).

⁵P. Ayyub, M. S. Multani, M. Barma, V. R. Palkar, and R. Vijayaraghavan, J. Phys. C **21**, 2229 (1988).

⁶T. Mitsuhashi, M. Ichihara, and U. Taksuke, J. Am. Ceram. Soc. **57**, 97 (1974).

⁷K. Uchino, E. Sadanaga, and T. Hirose, J. Am. Ceram. Soc. **72**, 1555 (1989).

⁸M. S. Multani, P. Guptasarma, V. R. Palkar, P. Ayyub, and A. V. Gurjar, Phys. Lett. A **142**, 293 (1989).

⁹P. E. D. Morgan, H. A. Bump, E. A. Pugar, and J. J. Ratto, in

Science of Ceramic Processing, edited by L. L. Hench and D. R. Ulrich (Wiley, New York, 1986), p. 327.

¹⁰Y. G. Wang, W. L. Zhong, and P. L. Zhang, Solid State Commun. **90**, 329 (1993); W. L. Zhong, Y. G. Wang, P. L. Zhang, and B. D. Qu, Phys. Rev. B **50**, 698 (1994).

¹¹K. Ishikawa, K. Yoshikawa, and N. Okada, Phys. Rev. B **37**, 5852 (1988).

¹²J. G. Bednorz and K. A. Müller, Z. Phys. B **64**, 189 (1986).

¹³H. G. Drickamer, in *Solid State Physics: Advances in Research and Applications Vol. 17*, edited by F. Seitz, D. Turnbull, and H. Ehrenfest (Academic, New York, 1965), p. 1.

¹⁴S. Hayashi and H. Abe, Jpn. J. Appl. Phys. **23**, L824 (1984).